JOURNAL OF THE KOREAN ASTRONOMICAL SOCIETY
39: 41 ~ 50, 2006

A PHOTOMETRIC STUDY OF THE CONTACT BINARY XZ LEONIS

JAE WOO LEE[1], CHUNG-UK LEE[2], CHUN-HWEY KIM[3], AND YOUNG WOON KANG[1]
[1]Astrophysical Research Center for the Structure and Evolution of the Cosmos,
Sejong University, Seoul 143-747, Korea
E-mail: leejaewoo@sejong.ac.kr & kangyw@sejong.ac.kr
[2]Korea Astronomy and Space Science Institute, Daejeon 305-348, Korea
E-mail: leecu@kasi.re.kr,
[3]Department of Astronomy and Space Science, College of Natural Science and Institute for
Basic Science Research, Chungbuk National University, Cheongju 361-763, Korea
E-mail: kimch@chungbuk.ac.kr
(Received May 22, 2006; Accepted June 21, 2006)

ABSTRACT

We present the results of new multi-color CCD photometry for the contact binary XZ Leo, together with reasonable explanations for the period and light variations. Six new times of minimum light have been determined. A period study with all available timings confirms Qian's (2001) finding that the O-C residuals have varied secularly according to $dP/dt = +8.20\times10^{-8}$ d yr^{-1}. This trend could be interpreted as a conservative mass transfer from the less massive cool secondary to the more massive hot primary in the system with a mass flow rate of about 5.37×10^{-8} $M_\odot$ yr^{-1}. By simultaneous analysis of our light curves and the previously published radial-velocity data, a consistent set of light and velocity parameters for XZ Leo is obtained. The small differences between the observed and theoretical light curves are modelled by a blue third light and by a hot spot near the neck of the primary component. Our period study does not support the tertiary light but the hot region which may be formed by gas streams from the cool secondary. The solution indicates that XZ Leo is a deep contact binary with the values of q=0.343, i=78°.8, Δ (T_1-T_2)=126 K, and f=33.6 %, differing much from those of Niarchos et al. (1994). Absolute parameters of XZ Leo are determined as follows: M_1=1.84 $M_\odot$, M_2=0.63 $M_\odot$, R_1=1.75 $R_\odot$, R_2=1.10 $R_\odot$, L_1=7.19 $L_\odot$, and L_2=2.66 $L_\odot$.

Key words : stars: binaries: close — stars: binaries: eclipsing — stars: individual (XZ Leo) — stars: spots

I. INTRODUCTION

XZ Leo (BD + 17°2165, HIP 49204, USNO-A2.0 1050-06187642) was discovered to be a short-period eclipsing binary by Hoffmeister (1934). Its character as a W UMa binary was revealed by the visual observations of Prichodko (1947) who also gave an improved light ephemeris. The only photoelectric light curves published so far were made by Hoffmann (1984) and radial-velocity curves of both components were obtained by Rucinski & Lu (1999, hereafter RL). Hoffmann's light curves show that sporadic light variations occur mainly in the two maxima (Max I and Max II; the maxima brightness following the primary and secondary eclipse, respectively) and Max II is slightly displaced to phase 0.76, while secondary minimum is shifted to phase 0.49. Niarchos et al. (1994, hereafter NHD) analyzed Hoffmann's BV light curves and concluded that the binary system is a hot, contact binary of spectral type A7 with the photometric parameters of q_{ph}=0.726, i=72°, Δ (T_1-T_2)=806 K, and f=7 %. In addition, they suggested that the light curves were better approximated by introducing one hot spot on each component near the neck region of the common envelope, and regarded this bright region as an effect of energy exchange between the components. However, their q_{ph} is very far from RL's spectroscopic mass ratio q_{sp}=0.348±0.029. The discrepancy could be caused partly by the unreliability of photometric mass ratios for partially eclipsing systems and/or possibly by third light reducing minimum depths (Pribulla et al. 2003). The orbital period of XZ Leo has been studied by NHD and Qian (2001). NHD reported that the period of 0.487735 d underwent a lengthening of about 0.14 sec in 1982, while Qian calculated a continuous period increase with the rate of $dP/dt = +8.79\times10^{-8}$ d yr^{-1} by assuming that the period of XZ Leo has suffered a parabolic variation.

A first spectral type of A5 for XZ Leo was determined by Hill & Schilt (1952). Later, Götz & Wenzel (1961) revised the classification to A7. Recently, NHD and RL deduced the spectral types to be A7~F0 and A8~F0 from analyses of photometric and spectroscopic measurements, respectively. The spectral classifications do not agree with the color index ($(B$-$V)$= +0.38±0.07) in the Hipparcos and Tycho Catalogues (ESA 1997), which would correspond to a spectral type of approximately F2. At present, no cause of the ap-

Corresponding Author: J. W. Lee

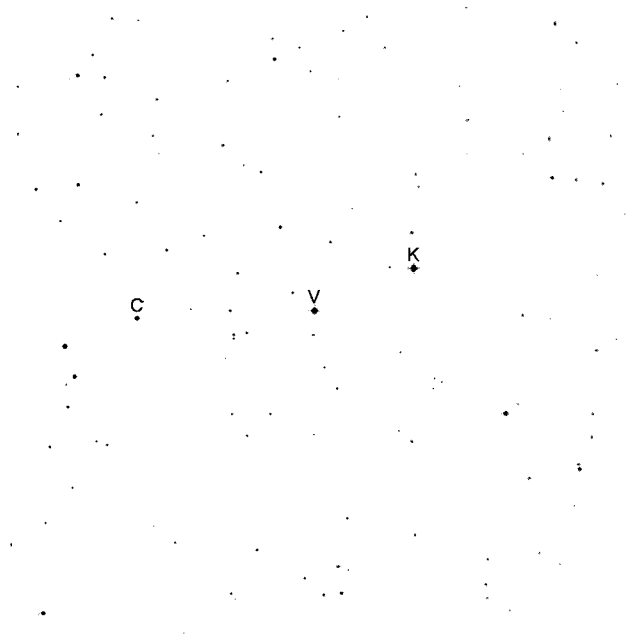

Fig. 1.— An observed CCD image (20′.5×20′.5) of XZ Leo (V), the comparison star (C), and the check star (K). The comparison star (USNO-A2.0 1050-06189275) does not appear on the map for XZ Leo in the Simbad data base. North is up and east is to the left.

parent disagreement between the spectral type and the color index is known. We note that the recent statistical studies (Pribulla et al.; Bilir et al. 2005) adopted the spectral type of A8V for the XZ Leo system.

To date, XZ Leo has been a quite neglected binary and thus most of its physical properties have been poorly known (e.g., the large difference between the photometric and spectroscopic mass ratios). In this paper, we present new *BVRI* light curves for the system and carry out a period study as well as a simultaneous analysis of light and radial velocity curves. Finally, based on our solution, an unique set of absolute parameters for the system is presented.

II. OBSERVATIONS

XZ Leo was observed on six nights from 25 February through 31 March 2005 in order to obtain precise multi-color light curves. The observations were carried out with a SITe 2K CCD camera and a standard Johnson *BVRI* filter set attached to the 61-cm reflector at Sobaeksan Optical Astronomy Observatory in Korea. The CCD chip has 2048×2048 pixels and a pixel size of 24μm, so the field of view (FOV) of a CCD frame is about 20′.5×20′.5 at the f/13.5 Cassegrain focus of the telescope. An observed image is given as Figure 1, wherein the variable is designated as "V". Since the FOV was large enough to observe a few tens of nearby stars simultaneously, we monitored them on each frame.

Using the customary IRAF package, we processed the frames to correct for bias level and flat fielding, and applied simple aperture photometry to get instrumental magnitudes of stars. Color, brightness and constancy in apparent light recommend USNO-A2.0 1050-06189275 ("C") and USNO-A2.0 1050-06186763 (GSC 1412-0423, "K"; K2) as comparison and check stars, respectively. The former is thought to be of mid-F spectral type from the color indices relative to XZ Leo and the check star, while the latter is much redder than the variable, although it has a brightness comparable to that of the binary system. Differential measurements with the check star indicated the constancy of the light of our comparison star throughout the observing runs, and the 1σ-values of an individual such measure are $0\overset{m}{.}013$, $0\overset{m}{.}011$, $0\overset{m}{.}012$ and $0\overset{m}{.}012$ from blue through infrared bandpasses. A total of 1310 individual observations was obtained in the four bandpasses (330 in *B*, 325 in *V*, 328 in *R*, and 327 in *I*; these designations do not denote *BVRI* standardizations) and are available upon request from the authors or through the Web page http://www.kasi.re.kr/∼ leecu/xzleo.photometry.obs.

III. PERIOD STUDY

Six times of minimum light were determined from our observations made during four primary and two secondary eclipses. All minima are the weighted means for the timings derived by the method of Kwee & van Woerden (1956) from the observations in the separate bandpasses. These are listed in Table 1, together with all photoelectric and CCD times of minimum light.

For our study of the period variability of XZ Leo, a total of 80 times of minimum light (16 photographic plate, 16 visual, 32 photoelectric and 16 CCD) have been collected from the data base of Kreiner et al. (2001) and from the more recent literature. To form an initial *O-C* diagram of the system, we used the light elements of Kreiner et al.:

$$C_1 = \text{HJD } 2445025.363 + 0.4877355E. \quad (1)$$

The resulting O–C_1 residuals calculated with this ephemeris are listed in the third column of Table 1 and drawn in the upper panel of Figure 2, where the times of minimum are marked by assorted symbols differing in size and shape according to observational method and type of eclipse. In our subsequent period analysis, one timing (HJD 2452274.5538), which is indicated by the arrow in the upper panel, was not used because its residual shows an unreasonably large deviation of -0.04 d compared to neighboring ones. We assigned weights of 10 to photoelectric and CCD minima, 5 to one normal minimum (HJD 2433011.702; Ashbrook 1952), and 1 to all others.

A linear least-squares fit to all photoelectric and CCD timings resulted in the following improved ephemeris to phase our photometric and RL's spectroscopic data (1σ-values follow each coefficient):

$$C_2 = \text{HJD } 2445025.3510(6) + 0.48773770(5)E. \quad (2)$$

TABLE 1.

OBSERVED PHOTOELECTRIC AND CCD TIMES OF MINIMUM LIGHT FOR XZ LEO

HJD (2400000+)	Epoch	O–C_1	O–C_2	O–C_3	Method[a]	Min	References
45025.358	0.0	-0.0050	0.0070	0.0040	PE	I	Hoffmann (1983)
45025.595	0.5	-0.0119	0.0001	-0.0028	PE	II	Hoffmann (1983)
45044.371	39.0	-0.0137	-0.0018	-0.0047	PEB	I	Braune & Mundry (1982)
45055.3475	61.5	-0.0112	0.0006	-0.0023	PEB	II	Braune & Mundry (1982)
45732.8154	1450.5	-0.0079	0.0009	-0.0007	PE	II	Faulkner (1986)
45779.3971	1546.0	-0.0050	0.0036	0.0021	PEV	I	Hübscher & Mundry (1984)
46079.8407	2162.0	-0.0065	0.0008	-0.0002	PE	I	Faulkner (1986)
46177.3872	2362.0	-0.0071	-0.0002	-0.0010	PE	I	Hübscher et al. (1985)
46910.4568	3865.0	-0.0039	-0.0004	-0.0001	PEV	I	Keskin & Pohl (1989)
47609.3834	5298.0	-0.0023	-0.0019	-0.0009	PEV	I	Wunder et al. (1992)
47609.3858	5298.0	0.0001	0.0005	0.0015	PE	I	Hübscher et al. (1989)
47612.3106	5304.0	-0.0015	-0.0012	-0.0001	PE	I	Hübscher et al. (1989)
47613.5286	5306.5	-0.0028	-0.0025	-0.0014	PE	II	Hübscher et al. (1989)
47614.5059	5308.5	-0.0010	-0.0007	0.0004	PE	II	Hübscher et al. (1989)
47616.4582	5312.5	0.0004	0.0007	0.0017	PE	II	Hübscher et al. (1989)
48680.4545	7494.0	0.0017	-0.0028	-0.0010	PEB	I	Diethelm (1992)
48733.3760	7602.5	0.0039	-0.0009	0.0010	PEV	II	Hübscher et al. (1992)
49004.5572	8158.5	0.0041	-0.0018	0.0001	PE	II	Hübscher et al. (1993)
49400.3579	8970.0	0.0075	-0.0003	0.0018	PE	I	Hübscher et al. (1994)
49401.3321	8972.0	0.0062	-0.0015	0.0005	PE	I	Hübscher et al. (1994)
49439.3762	9050.0	0.0069	-0.0010	0.0010	PE	I	Hübscher et al. (1994)
49756.4050	9700.0	0.0077	-0.0017	0.0004	PE	I	Agerer & Hübscher (1996)
49776.4021	9741.0	0.0076	-0.0018	0.0002	PEB	I	Diethelm (1995)
50137.3277	10481.0	0.0089	-0.0021	-0.0001	PEB	I	Agerer & Hübscher (1996)
50137.5708	10481.5	0.0082	-0.0029	-0.0009	PE	II	Agerer & Hübscher (1996)
50175.3742	10559.0	0.0121	0.0008	0.0028	CCD	I	Agerer & Hübscher (1997)
51163.5287	12585.0	0.0144	-0.0013	0.0003	CCDV	I	Agerer & Hübscher (1999)
51222.5464	12706.0	0.0161	0.0002	0.0017	CCD	I	Agerer & Hübscher (2000)
51256.4434	12775.5	0.0155	-0.0006	0.0009	CCD	II	Agerer & Hübscher (2000)
51629.807	13541.0	0.0176	-0.0002	0.0010	CCD	I	Nelson (2001)
52274.5538	14863.0	-0.0219	...	...	CCDV	I	Csizmadia et al. (2002)
52322.3948	14961.0	0.0210	0.0001	0.0005	PE	I	Agerer & Hübscher (2003)
52680.3927	15695.0	0.0210	-0.0015	-0.0015	PE	I	Hübscher (2005)
52721.3633	15779.0	0.0218	-0.0009	-0.0009	PE	I	Agerer & Hübscher (2003)
52721.6096	15779.5	0.0243	0.0016	0.0015	PE	II	Agerer & Hübscher (2003)
53040.5894	16433.5	0.0251	0.0009	0.0004	PE	II	Hübscher (2005)
53079.6099	16513.5	0.0267	0.0024	0.0018	PE	II	Hübscher (2005)
53379.5708	17128.5	0.0303	0.0046	0.0035	PE	II	Albayrak et al. (2005)
53409.5621	17190.0	0.0259	0.0000	-0.0011	CCD	I	Hübscher et al. (2005)
53410.5389	17192.0	0.0272	0.0014	0.0002	CCD	I	Hübscher et al. (2005)
53427.1211	17226.0	0.0264	0.0005	-0.0007	CCD	I	This Paper
53428.0964	17228.0	0.0262	0.0003	-0.0009	CCD	I	This Paper
53429.0720	17230.0	0.0263	0.0004	-0.0007	CCD	I	This Paper
53432.9743	17238.0	0.0268	0.0008	-0.0004	CCD	I	This Paper
53433.2180	17238.5	0.0266	0.0007	-0.0005	CCD	II	This Paper
53445.4107	17263.5	0.0259	-0.0001	-0.0013	CCD	II	Hübscher et al. (2005)
53451.5041	17276.0	0.0226	-0.0034	-0.0046	CCD	I	Hübscher et al. (2005)
53461.0189	17295.5	0.0266	0.0005	-0.0007	CCD	II	This Paper

[a]Method: (PE) multiplier photocell, (PEB) multiplier photocell with blue filter only, (PEV) multiplier photocell with yellow filter only, (CCD) electronic camera, (CCDV) electronic camera with yellow filter only.

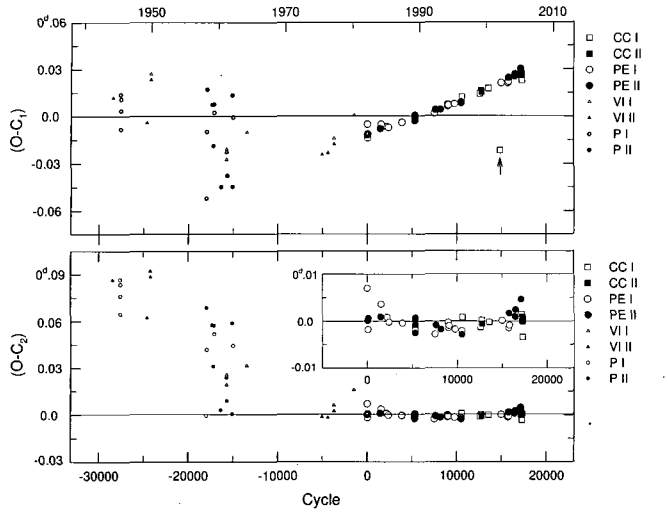

Fig. 2.— The upper panel shows the O–C_1 diagram of XZ Leo constructed with the light elements of Kreiner et al. (2001). One timing (HJD 2452274.5538) indicated by the arrow in the upper panel was not used in our subsequent analysis. The O–C_2 diagram from equation (2) obtained by least-squares fitting to all photoelectric and CCD timings is plotted in the lower panel, wherein a small box is drawn with only photoelectric and CCD residuals.

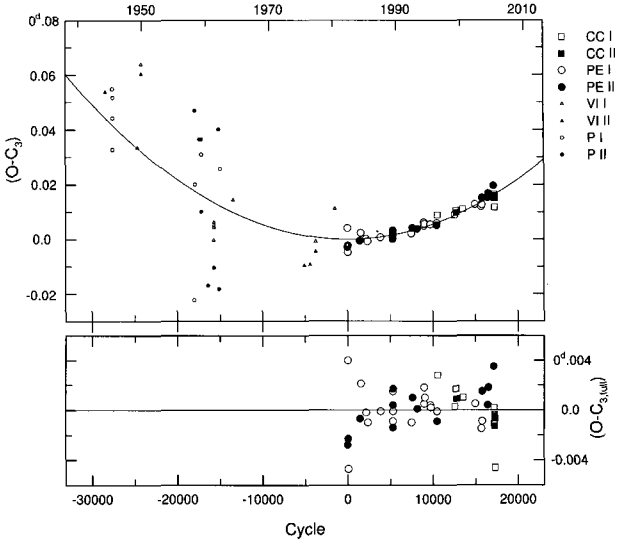

Fig. 3.— In the upper panel, the O–C_3 diagram of XZ Leo constructed with the linear terms of equation (3). The continuous curve represents the quadratic term of equation (3). The residuals of only photoelectric and CCD times of minimum light from the full equation (3) are plotted in the lower panel.

Based on the ephemeris (2), the O–C_2 residuals appear in the fourth column of Table 1 and are plotted in the lower panel of Figure 2. As shown in the figure, the general trend of all the O–C residuals from 1944 to 2005 can be represented by a parabola as assumed by Qian (2001). The parabolic pattern is also seen in only photoelectric and CCD residuals which are drawn in the small box of the lower panel. Thus, by introducing all times of minimum light into a parabolic least-squares fit, we obtained the following quadratic ephemeris:

$$C_3 = \mathrm{HJD}2445025.3540(1) + 0.48773665(1)E + 5.48(8) \times 10^{-11}E^2. \quad (3)$$

The 1σ-value for the last figure of each ephemeris parameter is given in parentheses. Our quadratic term and period are a little smaller than those of Qian. The O–C_3 residuals for this equation are given in the fifth column of Table 1. Figure 3 shows the O–C_3 diagram of XZ Leo constructed with the linear terms of equation (3). The continuous curve of the upper panel represents the quadratic term of equation (3) and the residuals of only photoelectric and CCD times of minimum light from the full ephemeris are plotted in the lower panel. As can be seen, the quadratic ephemeris provides a good fit to the mean trend of the O-C residuals, but the photoelectric and CCD residuals show short-term scatter of $\pm 0^{\mathrm{d}}.002$, which is about 4 times greater than the typical average precision ($\pm 0^{\mathrm{d}}.0005$) of times of minima determined from photoelectric or CCD photometry. This may indicate the existence of a (or some) further effect(s) producing the small scatter. In order to examine whether the residuals represent periodic variability, we used the Lomb-Scargle periodogram (Lomb 1976; Scargle 1982) as implemented in the software package supplied by Press et al. (1992), but no detectable periodicity was found. Hence, the scatter may be produced by the eclipse light curves' sporadic asymmetries due to stellar activity such as a starspot (Kalimeris et al. 2002) and/or the method of measuring the times of minima (van't Veer 1973; Maceroni & van't Veer 1994). The magnitude of this noise is annoyingly large; for instance, the timings of the cool contact binary BX Peg change by no more than 0.0008 d in absolute value (Lee et al. 2004).

The coefficient of the quadratic term in equation (3) is positive and indicates a continuous period increase with a rate of $\mathrm{d}P/\mathrm{d}t = +8.20\times10^{-8}$ d yr^{-1}. Such an apparent variation is not unusual for contact binaries. It is conventional to interpret such an increase as a conservative mass transfer from the less massive secondary star to the more massive primary component. With the masses of the primary and secondary components, which are obtained later in this paper, we get a mass transfer rate of about 5.37×10^{-8} $M_\odot$ yr^{-1}.

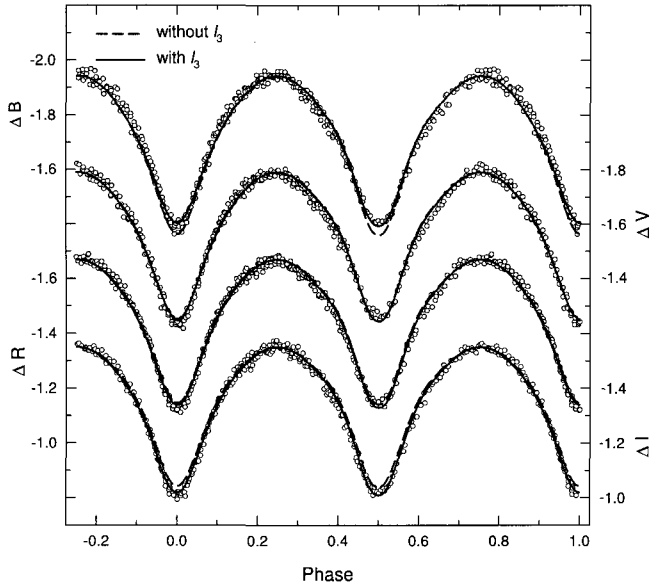

Fig. 4.— Light curves of XZ Leo in *BVRI* bandpasses as defined by individual observations. The dashed and solid curves are computed without and with l_3 adjustment, respectively. The synthetic light curves represent the results obtained by analyzing our light curves with the spectroscopic mass ratio (q=0.348). The theoretical light curves from the two solutions can be distinguished over only very limited phase intervals near the minima.

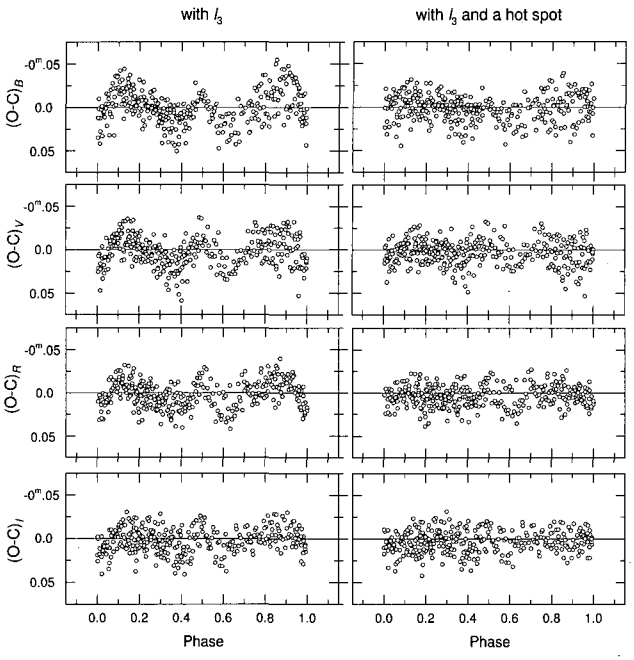

Fig. 5.— The corresponding residuals in B, V, R and I from two binary models: without (left panels) and with (right panels) the inclusion of a hot spot on the primary component. See text.

IV. LIGHT AND VELOCITY SOLUTIONS

The new *BVRI* light curves of XZ Leo phased by equation (2) are plotted in Figure 4 as magnitude differences (i.e., variable minus comparison star) versus phase. The brightness varies continuously as expected for a contact binary, and the curved shapes around both minima indicate partial eclipses. As may be seen in Figure 4, our light curves do not show the O'Connell effect of unequal light levels at the quadratures beyond the limits of the observational error of about ±0.01 mag. The light maxima (Max I and Max II) are displaced to around phases 0.24 and 0.76, which may be due to local photospheric inhomogeneities. Hoffmann's (1984) observations also indicated that brightness disturbances occur mainly in the two maxima and his Max II is slightly displaced to phase 0.76.

The latest Wilson-Devinney code (Wilson & Devinney 1971, hereafter WD) was adopted to solve our *BVRI* light curves simultaneously with the double-lined radial-velocity curves of RL. In these analyses, we employed all individual points using the contact mode 3 of the WD program and defined he subscripts 1 and 2 as the more massive hot star and the less massive cool component, respectively. Because there is essentially no interstellar extinction at the galactic coordinate (ℓ=218°.44 and b=49°.80) of XZ Leo from the reddening map of Burstein & Heiles (1982), we cannot resolve the conflict between the spectral classifications (A8∼F0V, RL; A7V, NHD) and the color ($(B-V)$=+0.38, ESA 1997). Thus, the temperature (T_1) of the primary star was assumed to be 7160 K averaged from Harmanec's (1988) and Flower's (1996) tables corresponding to the spectral type A8V by the spectroscopy and the color index in the Hipparcos and Tycho Catalogues.

] The gravity-darkening exponents and the bolometric albedos were fixed at standard values of g_1=g_2=1.0 and A_1=A_2=1.0, because each component should have a radiative envelope or at most a shallow convective atmosphere. The linear bolometric (X_1=X_2) and monochromatic (x_1=x_2) limb-darkening coefficients were adopted from the values of van Hamme (1993) in concert with the model atmosphere option. Other initial photometric parameters (the orbital inclination i, the temperature T_2 of the secondary star, the dimensionless surface potentials Ω_1=Ω_2 and the luminosity L_1) were estimated from the light curve (LC) part of the WD code. Throughout the analysis, synchronous rotation for both components (F_1=F_2=1) and a circular orbit (e=0) were accepted. Also, the method of multiple subsets (Wilson & Biermann 1976) was employed to reduce the intricacy of the correlations among parameters in a given iteration.

Our analyses of the light and velocity curves have

TABLE 2.
LIGHT AND VELOCITY CURVE PARAMETERS FOR XZ LEO

Parameter	Model 1		Model 2	
	Primary	Secondary	Primary	Secondary
ϕ_{sp}[a]	...		-0.0076(27)	
γ (km s^{-1})	...		-0.58(1.47)	
a ($R_\odot$)	...		3.519(31)	
q	0.348[b]		0.343(7)	
ϕ_{ph}[a]	0.0004(2)		0.0004(2)	
i (deg)	78.63(9)		78.77(9)	
T (K)	7160[b]	7035(4)	7160[b]	7034(4)
Ω	2.499(2)	2.499	2.488(2)	2.488
f (%)	33.4		33.6	
X	0.469[b]	0.469[b]	0.469[b]	0.469[b]
x_B	0.601[b]	0.601[b]	0.601[b]	0.601[b]
x_V	0.522[b]	0.522[b]	0.522[b]	0.522[b]
x_R	0.419[b]	0.419[b]	0.419[b]	0.419[b]
x_I	0.336[b]	0.336[b]	0.336[b]	0.336[b]
$L/(L_1+L_2+L_3)_B$	0.667(3)	0.244	0.670(4)	0.242
$L/(L_1+L_2+L_3)_V$	0.690(3)	0.255	0.694(4)	0.255
$L/(L_1+L_2+L_3)_R$	0.703(3)	0.263	0.707(4)	0.262
$L/(L_1+L_2+L_3)_I$	0.722(3)	0.272	0.725(4)	0.271
$l_{3,B}$[c]	0.089(3)		0.088(4)	
$l_{3,V}$[c]	0.055(3)		0.053(4)	
$l_{3,R}$[c]	0.034(3)		0.032(4)	
$l_{3,I}$[c]	0.006(3)		0.005(4)	
r (pole)	0.4583(3)	0.2873(4)	0.4595(3)	0.2861(4)
r (side)	0.4946(5)	0.3016(4)	0.4962(4)	0.3004(4)
r (back)	0.5261(6)	0.3475(8)	0.5275(6)	0.3463(8)
Colatitude (deg)	83.6(1.6)	...	83.6(1.6)	...
Longitude (deg)	1.4(6)	...	1.4(6)	...
Radius (deg)	13.2(5)	...	13.2(5)	...
$T_{\rm spot}/T_{\rm local}$	1.40(4)	...	1.40(4)	...

[a] ϕ_{sp} and ϕ_{ph} represent the phase shifts from spectroscopic and photometric data phased by equation (2), respectively.
[b] fixed parameter.
[c] Value at phase 0.25.

been carried out through two stages: at the first stage (hereafter Model 1) the light curves alone were solved with RL's spectroscopic mass ratio. In the second (hereafter Model 2), the light curves and RL's radial velocity data were simultaneously analyzed by using the system parameters of Model 1 as the initial values.

The result for Model 1 was shown as the dashed curves in Figure 4, where they do not fit well both of the eclipse minima as well as both of the descending and ascending branches for each eclipse. The observed eclipses are shallower than the computed ones in the blue bandpass, while they are deeper in the infrared one. The fact that the differences of eclipse depths between the observed and computed light curves could be dependent on bandpasses may suggest a third light in the system. Thus, we reanalyzed our light curves by considering a third light (l_3) as an additional adjustable parameter. The solutions reveal l_3 contributing 8.9% light in the B bandpass, 5.5% in V, 3.4% in R, and 0.6% in I. These are represented as the solid curves in Figure 4 giving a better fit. At this point, the residuals from the binary model with the third light were calculated to see the details of non-modelled lights and plotted in the left panel of Figure 5 where the quasi-sinusoidal variation pattern of the residuals is clearly seen, especially in the descending and ascending branches for each eclipse.

In many other contact binaries, such a feature has been reported and ascribed to surface inhomogeneities, such as magnetic stellar cool spot(s) on a component with a deep outer convective envelope and/or a hot spot due to a mass-transfer between the components (cf. Maceroni & van't Veer 1993). Therefore, an attempt to make a better fit was made with a single hot or cool spot on either of the components. The results are listed as Model 1 of Table 2 together with the spot parameters and the residuals from our binary model are plotted in the right panel of Figure 5 where we see that a hot spot near the neck of the primary component is sufficient to fit the light excess (or deficit) in

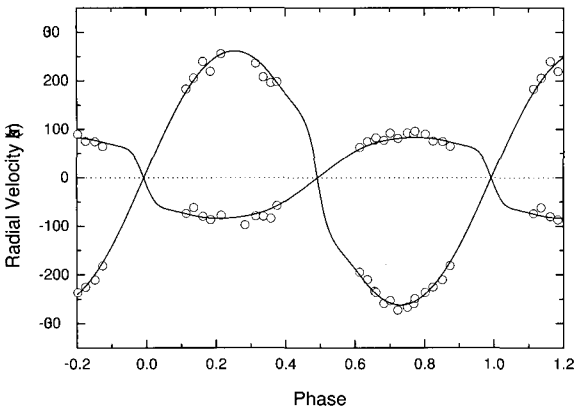

Fig. 6.— The radial-velocity curves of XZ Leo. The open circles are the measurements of RL, while the continuous curves denote the result from consistent light and velocity curve analysis including proximity effects.

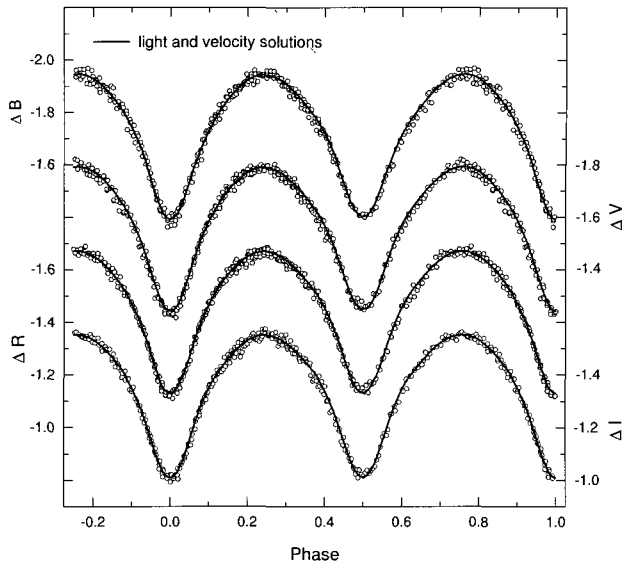

Fig. 7.— In the same sense as Figure 4, the continuous curves represent the corresponding solutions obtained with our model parameters in Model 2 of Table 2.

the descending and ascending branches. Separate trials for the other spot configurations were not so successful as for a hot spot on the primary star. There seems no need to posit more than one spot to fit our light curves. Because the XZ Leo system should have a common radiative envelope, as surmised from its spectral type, it is not reasonable to imagine solar-type magnetic spots on the components of the system. Hence, it seems more likely that the hot spot may be caused by a mass transfer from the less massive secondary star onto the more massive primary component inferred from our period study. In the process, the matter in transit through the neck of Roche lobes is accelerated and causes a shock wave, which heats the photosphere near the neck region of the accreting star and forms a hot spot on its surface (Lu 1991). On the other hand, we evaluated the spot behavior before searching for third light and found that, in result, the photometric parameters are in excellent agreement with Model 1 within their errors yielded by the WD code.

In the second stage, we analyzed our light curves and RL's radial velocity curves together. In principle, light and radial velocity curves can be always solved simultaneously, but usually it is not easy to assign relative weights reasonably to two totally different kinds of observations. It is still more difficult if the spot activity is variable with time and if the radial velocity measurements were not taken contemporaneously with the photometric ones. To avoid this, we analyzed light and radial velocity curves separately through two analysis steps. First, we analyzed only the radial velocity curves with the photometric solutions from Model 1. In the second step, only the light curves were solved by using the spectroscopic parameters obtained in the first. These processes were repeated until the two data sets were satisfied together (i.e., the correction of each parameter becomes smaller than its standard deviation). For all iterations, the mass ratio was treated as an adjustable parameter. The final results are listed as Model 2 in Table 2. The synthetic radial velocity curves are given in Figure 6, while the synthetic light curves are plotted in Figure 7. These plots show that our model fits two kinds of observations quite well.

V. DISCUSSION AND CONCLUSION

In this paper, we have obtained and analyzed new *BVRI* CCD observations of the A-subtype (defined observationally by Binnendijk (1970)) contact binary XZ Leo, of which physical properties have been poorly known. Our results represent the system as a deep contact binary with a small temperature difference of $\Delta(T_1\text{-}T_2)$=126 K between the components and with a relatively large fill-out factor of f=33.6 %, unlike the photometric parameters of NHD. The binary model with a third light and a single hot spot on the primary component fits the observed multi-color light curves quite well. If the third light is that of a tertiary companion gravitationally bound to the XZ Leo system, this object would be a white dwarf star as deduced from its color indices and can not be detected in RL's spectrograms due to its faintness. Because our period study gives no evidence for any third body in the system at the moment, the third light may come from a third star which is only optically related with XZ Leo. If the case is true, its source is likely to be a background blue star further than the binary system. The hot spot could be

TABLE 3.
ABSOLUTE PARAMETERS OF XZ LEO

Parameter	Primary	Secondary
M ($M_\odot$)	1.84(4)	0.63(2)
R ($R_\odot$)	1.75(2)	1.10(1)
log g (cgs)	4.22(1)	4.15(2)
T (K)[a]	7160(200)	7034(200)
L ($L_\odot$)	7.19(82)	2.66(31)
M_{bol} (mag)	2.60(12)	3.68(13)
B.C. (mag)	0.03	0.03
M_V (mag)	2.57(12)	3.65(13)
Distance (pc)	479(27)	

[a] Errors in both temperatures were assigned according to the uncertainty in the spectral type.

caused by gas streams from the less massive secondary that impact the inner hemisphere of the more massive primary component, an idea which agrees well with a conservative mass transfer from the secondary to the primary suggested by our period analysis.

The simultaneous analysis of light and velocity curves allows us to compute the absolute parameters listed in Table 3, where the radii (R) are the mean-volume radii evaluated using tabulations of Mochnacki (1984). The luminosity (L) and the bolometric magnitudes (M_{bol}) were obtained by adopting $T_{eff\odot}$=5777 K and $M_{bol\odot}$=$4^m.74$ for solar values (Cox 2000). To estimate the uncertainty in the luminosity, since the temperature error given in Table 2 is probably an underestimate, it was assumed that the temperature of each component had an error of 200 K in accordance with the unreliability in the spectral classification. For the absolute visual magnitudes (M_V), we used the bolometric corrections from Flower (1996) appropriate for the effective temperatures of the components. V=$10^m.60$ for the apparent visual magnitude at maximum light (Pribulla et al. 2003; Bilir et al. 2005) and our computed light ratio at phase 0.25 lead to V_1=$11^m.00$, V_2=$12^m.08$, and V_3=$13^m.79$ for the primary, secondary and tertiary stars, respectively. Ignoring the interstellar reddening (A_V=0), and using the values of V_1 and $M_{V,1}$ for the primary star, we have calculated the distance of the system to be 479±27 pc. This is too small compared with 1613 pc taken by the trigonometric parallax (0.62±1.71 mas) from the Hipparcos and Tycho Catalogues, while it is a little more distant than 386 pc computed from the photometric parallax of 2.59±0.32 mas (Bilir et al. 2005). The difference may partly result from the large uncertainty of the Hipparcos measurements for the XZ Leo system.

The computed absolute parameters of XZ Leo are used to estimate the evolutionary status of the system in the mass-radius, mass-luminosity and HR diagrams given by Hilditch et al. (1988). In these diagrams, the primary component of the system appears to be among the larger and more luminous primaries of contact binaries. The secondary is larger and brighter than expected for a ZAMS mass in the first two diagrams but its location on the HR diagram is to the left of the main-sequence band. This can be explained as a result of luminosity transfer from the primary to secondary component, as suggested by Hilditch et al. Since the derived masses and radii do not significantly depend upon the adopted effective temperatures, the mass-radius diagram was considered to be the principal indicator of the evolutionary status of the components. In this diagram, the primary star lies between ZAMS and TAMS and the secondary is slightly beyond TAMS, a location where the secondaries of some other A-subtype W UMa systems are found.

From the analysis of the O–C diagram, the orbital period of XZ Leo indicates a continuous period increase with a rate of $dP/dt = +8.20\times10^{-8}$ d yr^{-1}, which can be explained by mass transfer from the secondary to the primary component. According to the thermal relaxation oscillation (TRO) theory (Lucy 1976; Lucy & Wilson 1979), W UMa-type contact binaries like XZ Leo must oscillate cyclically between contact and non-contact conditions. In a state evolving from contact to non-contact phases, mass moves from the less massive secondary toward the more massive primary star, which is opposite to the energy flow, and an orbital period increase occurs. If the period and light variations of XZ Leo indicate just these circumstances, the system, at present, is in an expanding TRO state before broken-contact phase, as suggested by Qian (2001).

ACKNOWLEDGEMENTS

The authors wish to thank Professor R. H. Koch for careful readings and corrections and for some helpful comments of the original version of the manuscript. We have used the Simbad data base maintained at CDS many times and appreciate its availability. This work was supported by the Astrophysical Research Center for the Structure and Evolution of the Cosmos (ARCSEC) funded by the Korea Science and Engineering Foundation. CHK acknowledges partial support by Korea Research Foundation Grants (KRF-2005-015-C00188).

REFERENCES

Agerer, F. & Hübscher, J., 1996, Photoelectric Minima of Selected Eclipsing Binaries, Inf. Bull. Variable Stars, No. 4383

Agerer, F. & Hübscher, J., 1997, Photoelectric Minima of Selected Eclipsing Binaries and Maxima of Pulsating Stars, Inf. Bull. Variable Stars, No. 4472

Agerer, F. & Hübscher, J., 1999, Photoelectric Minima of

Selected Eclipsing Binaries, Inf. Bull. Variable Stars, No. 4711

Agerer, F. & Hübscher, J., 2000, Photoelectric Minima of Selected Eclipsing Binaries and Maxima of Pulsating Stars, Inf. Bull. Variable Stars, No. 4912

Agerer, F. & Hübscher, J., 2003, Photoelectric Minima of Selected Eclipsing Binaries, Inf. Bull. Variable Stars, No. 5484

Albayrak, B., et al., 2005, Photoelectric Minima of Some Eclipsing Binary Stars, Inf. Bull. Variable Stars, No. 5649

Ashbrook, J., 1952, Observed Times of Minimum of Eclipsing Variables, AJ, 57, 63

Bilir, S., Karataş, Y., Demircan, O., & Eker, Z., 2005, Kinematics of W Ursae Majoris Type Binaries and Evidence of the Two Types of Formation, MNRAS, 357, 497

Binnendijk, L., 1970, The Orbital Elements of W Ursae Majoris Systems, Vistas in Astronomy, 12, 217

Braune, W. & Mundry, E., 1982, Beobachtungsergebnisse der BAV (15th Compilation with Observations 1981-1982), BAV Mitt., No. 34

Burstein, D. & Heiles, C., 1982, Reddenings Derived from H I and Galaxy Counts: Accuracy and Maps, AJ, 87, 1165

Cox, A. N., 2000, Allen's Astrophysical Quantities (New York: Springer-Verlag)

Csizmadia, S., Zhou, A. Y., Konyves, V., Varga, Z., & Sandor, Z., 2002, Times of Minima of Eclipsing Binaries, Inf. Bull. Variable Stars, No. 5230

Diethelm, R., 1992, 133. List of Minima of Eclipsing Binaries, BBSAG Bull., No. 100

Diethelm, R., 1995, 141. List of.Minima of Eclipsing Binaries, BBSAG Bull., No. 108

ESA. 1997, The Hipparcos and Tycho Catalogues (ESA SP-1200; Noordwijk: ESA)

Götz, W. & Wenzel, W., 1961, Mitt. veränd. Sterne Sonneberg, No. 530

Faulkner, D. R., 1986, Epochs of Minimum Light for 27 Eclipsing Binaries, PASP, 98, 690

Flower, P. J., 1996, Transformations from Theoretical Hertzsprung-Russell Diagrams to Color-Magnitude Diagrams: Effective Temperatures, B-V Colors, and Bolometric Corrections, ApJ, 469, 355

Harmanec, P., 1988, Stellar Masses and Radii Based on Modern Binary Data, Bull. Astron. Inst. Czech., 39, 329

Hilditch, R. W., King, D. J., & McFarlane, T. M., 1988, The Evolutionary State of Contact and Near-Contact Binary Stars, MNRAS, 231, 341

Hill, S. J. & Schilt, J., 1952, Photographic Magnitudes of 55700 Stars in the Zones 10 deg to 20 deg and 30 deg to 50 deg, Contr. Rutherfurd Obs. Columbia Univ., No. 32

Hoffmann, M., 1983, Minima of W UMa Stars, Inf. Bull. Variable Stars, No. 2344

Hoffmann, M. 1984, Photoelectric Observations of Contact Binary Stars, Veröff. Astr. Instr. Bonn, 96

Hoffmeister, C., 1934, 132 neue Veräderliche, Astron. Nachr. 253, 195

Hübscher, J., 2005, Photoelectric Minima of Selected Eclipsing Binaries and Maxima of Pulsating Stars, Inf. Bull. Variable Stars, No. 5643

Hübscher, J., Agerer, F., & Wunder, E., 1992, Beobachtungsergebnisse der BAV (25th Compilation with Observations 1991-1992), BAV Mitt., No. 60

Hübscher, J., Agerer, F., & Wunder, E., 1993, Beobachtungsergebnisse der BAV (26th Compilation with Observations 1992-1993), BAV Mitt., No. 62

Hübscher, J., Agerer, F., & Wunder, E., 1994, Beobachtungsergebnisse der BAV (27th Compilation with Observations 1993-1994), BAV Mitt., No. 68

Hübscher, J., Lichtenknecker, D., & Munder, E., 1985, Beobachtungsergebnisse der BAV (18th Compilation with Observations 1984-1985), BAV Mitt., No. 39

Hübscher, J., Lichtenknecker, D., & Wunder, E., 1989, Beobachtungsergebnisse der BAV (22th Compilation with Observations 1988-198992), BAV Mitt., No. 52

Hübscher, J. & Mundry, E., 1984, Beobachtungsergebnisse der BAV (17th Compilation with Observations 1983-1984), BAV Mitt., No. 38

Hübscher, J., Paschke, A., & Walter, F., 2005, Photoelectric Minima of Selected Eclipsing Binaries and Maxima of Pulsating Stars, Inf. Bull. Variable Stars, No. 5657

Kalimeris, A., Rovithis-Livaniou, H., & Rovithis, P., 2002, Starspots and Photometric Noise on Observed Minus Calculated (O-C) Diagrams, A&A, 387, 969

Keskin,V. & Pohl.E., 1989, Photoelectric Minima of Eclipsing Binaries, Inf. Bull. Variable Stars, No. 3355

Kreiner, J. M., Kim, C.-H., & Nha, I.-S., 2001, An Atlas of O-C Diagrams of Eclipsing Binary Stars (Krakow: Wydawn. Nauk. Akad. Pedagogicznej)

Kwee, K. K., & van Woerden, H. 1956, A Method for Computing Accurately the Epoch of Minimum of an Eclipsing Variable, Bull. Astron. Inst. Netherlands, 12, 327

Lee, J. W., Kim, C.-H., Han, W., Kim, H.-I., & Koch, R. H. 2004, Period and Light Variations for the Cool, Overcontact Binary BX Pegasi, MNRAS, 352, 1041

Lomb, N. R., 1976, Least-Squares Frequency Analysis of Unequally Spaced Data, Ap&SS, 39, 447

Lu, W., 1991, Radial-Velocity Observations and Absolute Dimensions of Eclipsing Binaries - SS Ari, AJ, 102, 262

Lucy, L. B., 1976, W UMa Systems with Marginal Contact, ApJ, 205, 208

Lucy, L. B., & Wilson, R. E., 1979, Observational Tests of Theories of Contact Binaries, ApJ, 231, 502

Maceroni, C. & van't Veer, F., 1993, The Uniqueness of Photometric Solutions for Spotted W Ursae Majoris Binaries, A&A, 277, 515

Maceroni, C. & van't Veer, F., 1994, Period Variations of the Late Type Contact Binaries YY Eri and AE Phe: How to Use Light Curves Outside Minimum, A&A, 289, 871

Mochnacki, S. W., 1984, Accurate Integrations of the Roche Model, ApJS, 55, 551

Nelson, R. H., 2001, CCD Minima of Selected Eclipsing Binaries in 2000, Inf. Bull. Variable Stars, No. 5040

Niarchos, P. G., Hoffmann, M., & Duerbeck, H. W., 1994, The Hot Contact Binary XZ Leonis, A&A, 292, 494

Press, W., Flannery, B. P., Teukolsky, S. A., & Verrerling, W. T., 1992, Numerical Recipes (Cambridge: Cambridge Univ. Press), chap. 13

Pribulla, T., Kreiner, J. M., & Tremko, J., 2003, Catalogue of the Field Contact Binary Stars, Contrib. Astron. Obs. Sk. Pleso, 33, 38

Prichodko, A., 1947, Variable Stars, 6, 135

Qian, S., 2001, Orbital Period Changes of Contact Binary Systems: Direct Evidence for Thermal Relaxation Oscillation Theory, MNRAS, 328, 914

Rucinski, S. M. & Lu, W., 1999, Radial Velocity Studies of Close Binary Stars. II, AJ, 118, 2451

Scargle, J. D., 1982, Studies in Astronomical Time Series Analysis. II - Statistical Aspects of Spectral Analysis of Unevenly Spaced Data, ApJ, 263, 835

Van Hamme, W., 1993, New Limb-Darkening Coefficients for Modeling Binary Star Light Curves, AJ, 106, 209

Van't Veer, F., 1973, The Eclipsing Contact Binary VW Cep, A&A, 26, 357

Wilson, R. E. & Biermann, P., 1976, TX Cancri - Which Component is Hotter, A&A, 48, 349

Wilson, R. E. & Devinney, E. J., 1971, Realization of Accurate Close-Binary Light Curves: Application to MR Cygni, ApJ, 166, 605

Wunder, E., Wieck, M., Kilinc, B., Gulmen, O., Tunca, Z., & Evren, S., 1992, New Photoelectric Minima of Some Eclipsing Binaries, Inf. Bull. Variable Stars, No. 3760